Allometric models of *Picea* spp. biomass for airborne laser sensing as related to climate variables

Allometric models of *Picea* spp. biomass for airborne laser sensing as related to climate variables

V Usoltsev[1,2], V Kovyazin[3*], I Tsepordey[2], S Zalesov[1] and V Chasovskikh[4]

[1]Institute of Forest and Natural Resource Management, *Ural State Forest Engineering University*, 37 SibirskyTrakt Street, Yekaterinburg 620100, Russian Federation
[2]Laboratory of Forest Ecology, *Botanical Garden, Ural Branch of the Russian Academy of Sciences*, 202a, 8 Marta Street, Yekaterinburg 620144, Russian Federation
[3]Department of Engineering Geodesy, *Saint Petersburg Mining University* 2, 21st Line Vasil, Saint- Petersburg 199106, Russian Federation
[4]Department of Chess Art and Computer Mathematics, *Ural State University of Economics*, 62, 8 Marta Street, Yekaterinburg 620144, Russian Federation

*Corresponding email: vfkedr@mail.ru

Abstract. Over the past two decades, active airborne laser sensing technology has been intensively used to scan the forest cover, providing such morphometric indicators of trees as the width and projection area of the crown, the height of the tree. The author's database of harvest data of 1550 model trees of genus *Picea* spp. of Eurasia is used in the work. Allometric models of biomass components, including the crown width, tree height, winter temperatures and precipitation as independent variables, are designed. The biomass of all components of equal-sized trees is described by the propeller-shaped 3D picture. In cold regions, when precipitation increases, the biomass decreases, but as one moves to cold regions, it is characterized by an opposite or neutral trend. As the temperature increases in humid regions, the biomass increases, but as the transition to dry conditions begins to decrease.

1. Introduction

Global forests comprise 80% of plant biomass [1] and exceed the planet's atmosphere in carbon content [2]. Over the past two decades, active airborne laser sensing (ALS) technology has been intensively used to scan forest cover, providing spatial and temporal characteristics that are unprecedented in accuracy and speed. Thanks to this, the technology provides highly accurate information about large areas of forests in a very short time. Due to the ability to penetrate through the thickness of the canopy, laser sensing data characterize its vertical structure, including the understorey [3, 4]. The results of laser sensing, representing three-dimensional point clouds, provide detailed information in three dimensions about the structure of the forest [5], allow us to make segmentation of individual trees and obtain their morphometric characteristics [6, 7]. Laser sensors measure the distance to trees, to their structural elements, and to the ground by recording the time interval between the emission and return of laser pulses [8]. ALS device is placed on the aircraft, the position of which is recorded using the differential global positioning system GPS and inertial measurement units [9].

Although remote sensing techniques for individual trees are less well understood compared to the achievements of traditional ground-based taxation [10], significant advances have been made in recent years in the field of individual tree detection and recording of crown shape and structure (crown width, tree height, projection area, and crown volume) based on new high-performance algorithms and the use of unmanned aerial vehicles (UAVs, or drones) [11-16].

The crown width indicator was used to estimate the aboveground biomass of multi-stemmed trees and shrubs instead of the trunk diameter, since in such cases the trunk diameter was not very informative and difficult to measure [17, 18]. In particular, for *Haloxylon* Bunge communities growing in the deserts of Central Asia, allometric models of the relationship of aboveground biomass with the height of the tree (bush) and the width of the crown were developed [19]

$$\ln P_a = a_0 + a_1 \ln H + a_2 \ln D_{\text{cr}} \quad (1)$$

where, P_a = aboveground biomass, kg; H = bush (tree) height, m; D_{cr} = crown width, m. Later, based on the aboveground biomass of 2635 *Haloxylon* trees taken from 100 sample plots established in the deserts of Kazakhstan, models (1) were calculated with determination coefficients from 0.841 to 0.854, intended for both remote and ground inventory of *Haloxylon* communities [20].

The inclusion of temperature and precipitation as additional independent variables in allometric models of biomass significantly improves the accuracy of estimates and makes it possible to predict changes in biomass during climate shifts [21, 22]. However, such sensitive to climate variables models are developed for aboveground biomass without division into components and do not take into account the contribution of climate variables to the explanation of the variability of tree biomass.

In this study we intend (1) when using the structure of biomass allometric model, we try reveal how the biomass components relate not only to morphometric indices of trees, namely, crown width and tree height, but also to temperature and humidity fluctuations on Eurasian territory and (2) what contribution to the explanation of the dispersion of biomass components have the morphometric indices of trees, and climatic variables.

2. Methods and Materials

To ask the above mentioned questions, we used the author's database of harvest data. The first version of the database consisted of 7330 trees [23], selecting from which 1006 trees, models (1) were calculated [24, 25]. The second version of the database already included 15 200 trees [26]. From the latest database, 1 550 *Picea* model trees were selected with measured tree height and foliage and branch biomass, crown width and length, and trunk biomass, 1 330 trees with trunk and aboveground biomass, 1 185 trees with crown length, 970 trees with crown width, and 400 trees with measured root biomass (table 1). The genus *Picea* spp. is mainly represented by *Picea abies* (L.) H. Karst. and *P.obovata* Ledeb.) and in a smaller number by *P. schrenkiana* F. *et* M., *P. ajanensis* (Lindl. *et* Gord.) Fisch. *ex* Carr., *P. koraiensis* Nakai. and *P. purpurea* Mast.

Table 1. Statistics of database samples for *Picea* trees in Eurasia.

Statistic designation[a]	Indices analyzed[b]							
	H	L_{cr}	D_{cr}	*Ps*	*Pb*	*Pf*	*Pa*	*Pr/Pa*
Mean	13.8	7.9	2.7	136.4	20.4	12.6	168.1	0.24
Min	0.43	0.70	0.25	0.005	0.001	0.004	0.011	0.065
Max	44.8	29.5	10.9	4122.0	1259.6	305.0	5089.0	0.81
SD	9.3	4.6	1.5	337.7	59.3	26.1	413.0	0.09
CV, %	67.6	58.8	55.8	247.6	291.0	206.9	245.7	38.8
n	1550.0	1185.0	970.0	1330.0	1550.0	1550.0	1330.0	400.0

[a]Mean = mean value; Min = minimum value; Max = maximum value; SD = standard deviation; CV = coefficient of variation; n = number of observations.
[b]*H* = tree height, m; L_{cr}= crown length, м; D_{cr}= crown width, m; *Ps, Pb, Pf, Pa, Pr* = stem over bark, branches, foliage, aboveground, root biomass in a completely dry condition correspondingly, kg.

Based on the analysis of previous studies, we are inclined to believe that the most informative independent variables in assessing the biomass of trees by remote sensing are the width of the crown and the height of the tree. We need to test how sensitive such an allometric model is to climate shifts.

For this purpose, the available data of geographical coordinates of model trees are plotted on the maps of mean January temperature (https://store.mapsofworld.com/image/cache/data/map_2014 /currents-and-temperature-jan-enlarge-900x700.jpg) and mean annual precipitation (http://www.mapmost.com/world-precipitation-map/free-world-precipitation-map/) [27] (figure 1) and were joint with morphometric indices of model trees [28]. The refusal to use the average annual

temperature in favor of the average January temperature was motivated earlier [29]. The resulting table of source data is included in the regression analysis procedure [30].

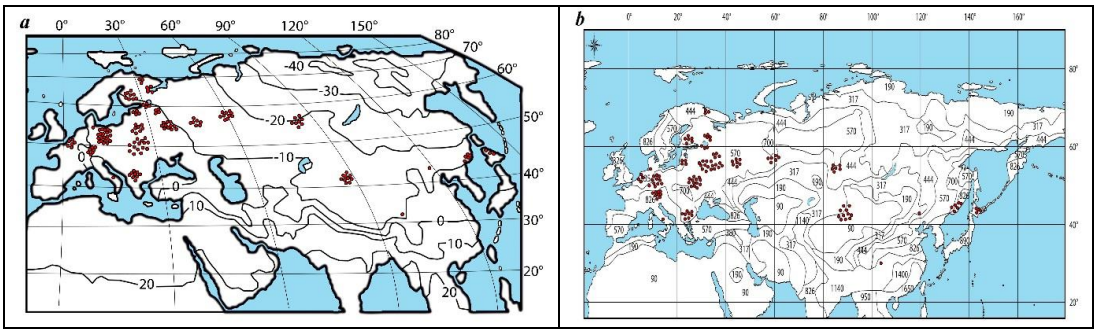

Figure 1. Distribution of biomass harvest data of 1550 spruce sample trees on the map of the mean January temperature, °C (*a*) and on the map of the mean annual precipitation, mm (*b*) [27].

3 Results and Discussion

For regression analysis, the following model structure is proposed, including both morphometric characteristics of trees and climatic indicators as independent variables:

$$\ln P_i = a_0 + a_1(\ln D_{cr}) + a_2(\ln H) + a_3[\ln(T+40)] + a_4(\ln PR) + a_5[\ln(T+40)]\cdot(\ln PR)) \quad (2)$$

where, T = average January temperature, °C; PR = average annual precipitation, mm; $[\ln(T{+}40)]\cdot(\ln PR)$ = combined variable that characterizes the combined effect of temperature and precipitation. Since the average temperature of January in high latitudes has a negative value, for its logarithmic transformation in the model (2), it is modified to the form (T+40). The results of the calculation of the models (2) are shown in table 2. Geometrical presentation of the models (2) gives figure 2.When tabulating, the average values of D_{cr} and H are used (table 1).

Table 2. The results of calculating models (2).

ln(*Y*)	a_0[(a)]	lnD_{cr}	ln*H*	ln(*T*+40)	ln*PR*	[ln(*T*+40)]× (ln*PR*)	adjR^{2}[(b)]	SE[(c)]
ln(*Ps*)	91.3762	0.6862	2.1229	-27.1626	-15.0636	4.3568	0.974	0.39
ln(*Pf*)	27.4702	1.2380	0.9116	-6.8624[(d)]	-5.0223	1.2126[(d)]	0.848	0.66
ln(*Pb*)	30.2767	1.6641	1.0806	-7.9246	-5.5036	1.3599	0.908	0.61
ln(*Pa*)	73.9962	0.9059	1.7195	-21.4481	-12.2168	3.4829	0.960	0.44

[(a)]The intercept hereafter is adjusted according to Baskerville's [31] logarithmic transformation;
[(b)]$adjR^2$= the coefficient of determination, adjusted for the number of variables;
[(c)]SE = the standard error of the equation;
[(d)]– these regression coefficients are not reliable at the level of p = 0.95.

As can be seen from table 1, the amount of harvest data on root biomass is three times less than of data on aboveground biomass, and this is a common property of all tree biomass databases [23, 24]. Due to the insufficient representation of our data on root biomass, we calculated models (2) for a relative indicator, namely, for the root/shoot ratio:

$$\ln(P_r/P_a) = 2.1956 + 0.3186(\ln D_{cr}) - 1.2247[\ln(T+40)];\ \text{adjR}^2 = 0.288;\ \text{SE} = 0.30. \quad (3)$$

The variability of the root/shoot ratio is explained by independent variables to the least extent (29%) compared to the components of aboveground biomass (table 2). The only statistically significant independent variables were crown width and average January temperature ($t = 5.1$ and $7.9 > t_{999} = 3.3$). A graphical interpretation of this relationship is shown in figure 3.

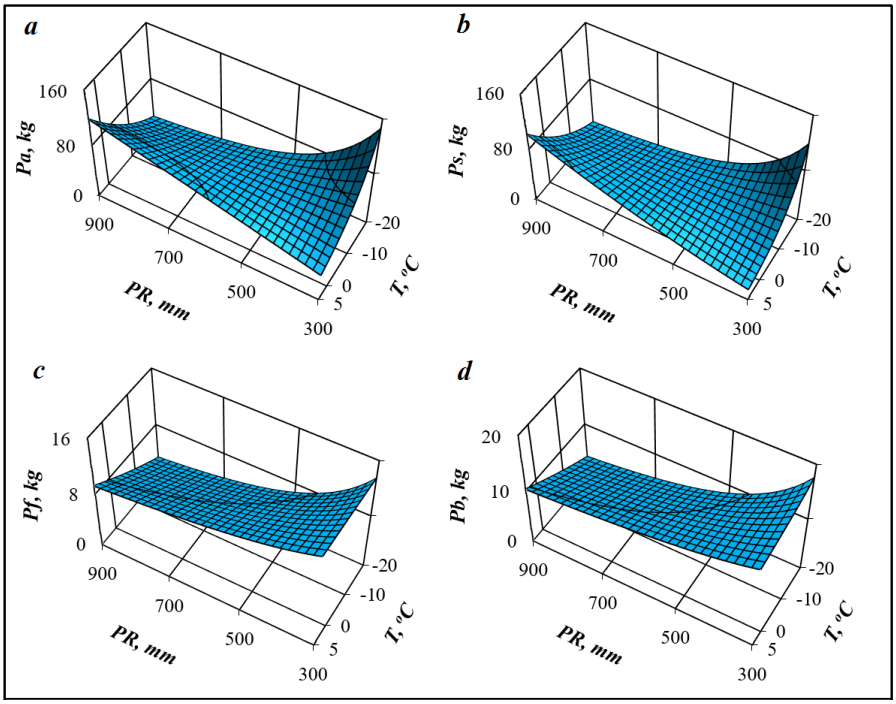

Figure 2. The theoretical changes in *Picea* spp. biomass components in relation to mean temperature of January (*T*) and mean rainfall (*PR*). Component designations: *a, b, c, d* – above ground, trunk, foliage and branch biomass, correspondingly.

As we can see in figure 2, the dependence of all components of the biomass of equal-sized spruce trees on temperature and precipitation is described by a propeller-shaped 3D picture. In cold regions, when precipitation increases, the biomass decreases, but as it moves to warm regions, it is characterized by an opposite or neutral trend. As the temperature increases in humid regions, the biomass increases, but as the transition to dry conditions begins to decrease. In other species, in particular, two-needled pines, oak or larch, the patterns are sometimes different, and sometimes opposite [25, 28, 29]. This seems to be related to the biological characteristics of tree species and to the distribution of tree assimilates into its various components [32].

As in previous publications on the biomass of two-needled pines [28] and larch [33], the root/shoot ratio of spruce trees increases as the negative temperatures of January increase, i.e. in the direction of high latitudes (figure 3). This conclusion is in accordance with the previously obtained patterns of other authors. In particular, in the latitudinal gradient from the Pacific coast of China (35°N) to the permafrost regions of Yakutia (67°N), the root/shoot ratio of larch forests increases from 0.09 to 1.20 [34]. On the territory of European Russia, the root/shoot ratio increases from 0.2 in the subtropics to 0.6 in the subarctic zone [35].

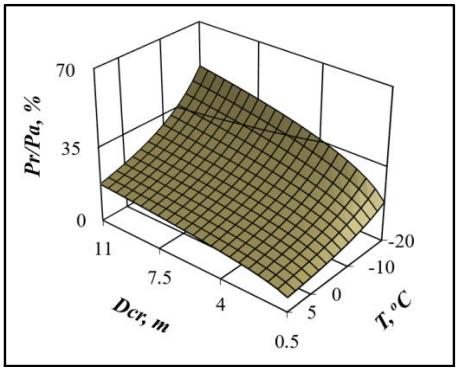

Figure 3. Change of the theoretical R/S ratio in relation to tree crown width under different mean January temperature (*T*).

To assess the stability of the model, it is necessary to have information about the contribution of independent variables to the explanation of the variability of the dependent variable. Based on the results of the regression analysis, table 3 is suggested for this purpose.

Table 3. Contribution of independent variables of models (2) to the explanation of variability of dependent variables, %.

ln(*Y*)	Independent variables						
	lnD_{cr} (I)	ln*H* (II)	I+II	ln(*Tm*+40) (III)	ln*PRm* (IV)	[ln(*Tm*+40)] × (ln*PRm*) (V)	III+IV+ V
ln(*Ps*)	13.8	57.6	71.4	9.4	9.6	9.6	28.6
ln(*Pf*)	42.8	42.7	85.5	4.3	5.5	4.7	14.5
ln(*Pb*)	46.3	40.6	86.9	3.9	4.9	4.3	13.1
ln(*Pa*)	20.8	53.1	73.9	8.5	8.8	8.8	26.1
X ± σ[(a)]	30.9±16.1	48.5±8.2	79.4±7.9	6.5±2.8	7.2±2.3	6.9±2.7	20.6±7.9

[(a)] X ± σ = mean ± standard deviation.

We can see in table 3 that climate variables explain the variability of trunk and aboveground biomass to the greatest extent (from 26 to 29 %) and needles and branches to the least extent (from 13 to 15%). Morphometric variables explain the variability of the biomass of needles and branches to the greatest extent (from 86 to 87%), and in the least one – trunks and aboveground (from 71 to 74%).

Since trees of different tree species have a specific configuration of the vertical profile, this specificity is now successfully recognized using airborne laser locators [36-38]. With multiple lidar registration of reflected laser pulses, the nature of the grouping of point clouds and its outline can be distinguished with 95% accuracy between pine, spruce and birch species. Pine differs from deciduous birch in the characteristic thickening of point clouds, and spruce differs from others in the shape of the crown [39-42]. At the current rate of development of laser and IT technology, it is possible that in the near future it will be possible to distinguish remotely even such visually similar species as spruce and fir. Lidar from a low-flying drone [16] will be able to distinguish spruce and fir by the opposite orientation of their cones, and ground-based lidar [43] will confirm this difference by the structure of the trunk bark (rough in spruce and smooth in fir).

Ground-based laser scanning of a forest stand can produce a value of the crown length, which, at a given tree height, characterizes the change in tree biomass due to local growing conditions: tree vigour [44], stand density, competition and survival potential of trees within a forest [45]. We introduced the crown length into the model (2) as an additional independent variable. It turned out that with the same size of the width of the crown and the height of the tree, an increase in the length of the crown has a positive effect on the biomass of all components. But this effect is statistically significant for the biomass of needles, branches, rootsand aboveground ($t = 3.2 \div 16.5 > t_{05}=1.96$), and not significant for the biomass of the trunk ($t = 1.3 < t_{05}=1.96$). The inclusion of the crown length in the model either does not increase the adequacy of the model or increases it by an insignificant amount - from 0.6 to 2.0 %.

4. Conclusions

Thus, an allometric model has been developed that describes the positive relationship of the biomass of all components of *Picea* trees with the crown width and tree height at the level of $p < 0.001$, which makes it possible to evaluate all components of the biomass by remote sensing methods with a high degree of accuracy.

The introduction of temperature and precipitation as additional independent variables into the allometric model showed that the biomass of equal-sized trees is described by a 3D picture. In cold regions, when precipitation increases, the biomass decreases, but as it moves to warm regions, it is characterized by an opposite or neutral trend. As the temperature increases in humid regions, the biomass increases, but as the transition to dry conditions begins to decrease. The discrepancy between the results obtained and previously published data for other species may be due to the biological characteristics of tree species and the distribution of photosynthetic products of a tree in its various components.

It was found that climate variables explain the variability of trunk and aboveground biomass to the greatest extent, and needles and branches to the least extent, and morphometric variables – on the contrary, respectively.

The results obtained can be useful in monitoring forest biomass based on laser sensing.

Acknowledgements
We thank the anonymous referees for their useful suggestions. This paper was prepared within the programs of the current scientific research of the Ural Forest Engineering University, Botanical Garden of the Ural Branch of Russian Academy of Sciences and Saint Petersburg Mining University.

References

[1] Kindermann G E, McCallum I, Fritz S and Obersteiner M 2008 A global forest growing stock, biomass and carbon map based on FAO statistics. *Silva Fennica*, **42** 387–96
[2] Pan Y *et al* 2011 A large and persistent carbon sink in the world's forests. *Science*, **333** 988–93
[3] Swatantran A, Tang H, Barrett T, DeCola P and Dubayah R 2016 Rapid, high-resolution forest structure and terrain mapping over large areas using single photon lidar. *Scientific Reports*, **6** 28277. DOI: 10.1038/srep28277
[4] Hamraz H, Contreras M A and Zhang J 2017 Forest understory trees can be segmented accurately within sufficiently dense airborne laser scanning point clouds. *Scientific Reports*, **7**(1) 6770. DOI: 10.1038/s41598-017-07200-0
[5] Dubayah R O and Drake J B 2000 Lidar remote sensing for forestry. *Journal Forestry*, **98** (6) 44-46
[6] Ayrey E, Fraver S, Kershaw Jr Ja, Kenefic L S, Hayes D, Weiskittel A R and Roth B E 2005 Layer stacking: A novel algorithm for individual forest tree segmentation from LiDAR point clouds. *Canadian Journal Remote Sensing*, **43** (1) 16-27
[7] Dalponte M 2018 *itcSegment: Individual tree crowns segmentation*. R package version 0.8. *Available at:* https://CRAN.R-project.org/package=itcSegment.
[8] Lefsky M A, Cohen W B, Parker G G and Harding D J 2003 Lidar remote sensing for ecosystem studies. *AIBS Bulletin*, **52** (1) 19-30
[9] Hyyppä J, Hyyppä H, Leckie D, Gougeon F, Yu X and Maltamo M 2008 Review of methods of small-footprint airborne laser scanning for extracting forest inventory data in boreal forests. *International Journal Remote Sensing*, **29** (5) pp1339-366
[10] Silva C A *et al* 2014 Imputation of individual longleaf pine (*Pinus palustris* Mill.) tree attributes from field and LiDAR data. *Canadian Journal of Remote Sensing*, **42** (5) 554-573
[11] Popescu S C, Wynne R H and Nelson R F 2003 Measuring individual tree crown diameter with lidar and assessing its influence on estimating forest volume and biomass. *Canadian Journal of Remote Sensing*, **29** (1) 564-577
[12] Goodwin N R, Coops N C and Culvenor D S 2006 Assessment of forest structure with airborne LiDAR and the effects of platform altitude. *Remote Sensing of Environment*, **103** 140–152. DOI:10.1016/j.rse.2006.03.003
[13] Dalponte M and Coomes D A 2016 Tree-centric mapping of forest carbon density from airborne laser scanning and hyperspectral data. *Methods Ecology Evolution*, **7** (10) pp 1236-245
[14] Zhen Z, Quackenbush L J and Zhang L 2016 Trends in automatic individual tree crown detection and delineation—Evolution of LiDAR data. *Remote Sensing*, **8** (4) p 333
[15] Silva C A, Crookston N L, Hudak A T, Vierling L E, Klauberg C and Cardil A 2017 *rLiDAR: LiDAR data processing and visualization*. R package version 0.1.1. *Available at:* https:// CRAN.R-project.org/package=rLiDAR.
[16] Neuville R, Bates J S and Jonard F 2021 Estimating forest structure from UAV-mounted LiDAR point cloud using machine learning. *Remote Sens*ing, **13** 352 DOI:10.3390/rs13030352
[17] Leontiev V L 1950 On the determination of the mass of *Haloxylon* Bunge. *Botanical Journal*, 35 (6) pp 637-645
[18] Ohmann L F, Grigal D F and Brander R B 1976 Biomass estimation for five shrubs from northeastern Minnesota. *USDA Forest Service, North Central Forest Experiment Station.* Research paper NC-133 p 11

[19] Veyisov S and Kaplin V G 1976 To the method of biomass estimating in white saxaul of the Eastern Kara-Kum desert. *Problems of desert exploitation* [In Russia - *Problemy osvoeniya pustyn'*], **1** 60–64
[20] Usoltsev V A 1990 Mensuration of forest biomass: Modernization of standard base of forest inventory. *Proceedings of the XIX World Congress, IUFRO, Division 4. Canada, Montreal* 79–92. Retrieved from: https://www.researchgate.net/publication/312094663_Usoltsev_V_A_Mensuration_of_forest_biomass_Modernization_of_standard_base_of_forest_inventory_XIX_World_Congress_Proceedings_IUFRO_Division_4_Canada_Montreal_1990-_P_79-92
[21] Zeng W S, Duo H R, Lei X D, Chen X Y, Wang X J, Pu Y and Zou W T 2017 Individual tree biomass equations and growth models sensitive to climate variables for *Larix* spp. in China. *European Journal of Forest Research*, **136** 233–249
[22] Fu L, Sun W and Wang G 2017 A climate-sensitive aboveground biomass model for three larch species in northeastern and northern China. *Trees*, **31** 557–573
[23] Usoltsev V A 2016a *Single-tree biomass of forest-forming species in Eurasia: Database, climate-related geography, weight tables*. Yekaterinburg, Ural State Forest Engineering University. pp 336. ISBN 978-5-94984-568-4. *Retrieved from*: https://elar.usfeu.ru/handle/123456789/5696
[24] Usoltsev V A 2016b *Single-tree biomass data for remote sensing and ground measuring of Eurasian forests*. CD-version in English and Russian. Yekaterinburg: Ural State Forest Engineering University. *Available at*: http://elar.usfeu.ru/bitstream/123456789/6103/1/Usoltsev_%20Database_en_16.xlsx
[25] Usoltsev V A, Shobairi S O R, Chasovskikh V P 2019a Comparing of allometric models of single-tree biomass intended for airborne laser sensing and terrestrial taxation of carbon pool in the forests of Eurasia. *Natural Resource Modeling*, **32** e12187. DOI: 10.1111/nrm.12187
[26] Usoltsev V A 2020 *Single-tree biomass data for remote sensing and ground measuring of Eurasian forests: digital version*. The second edition, enlarged. Yekaterinburg, Ural State Forest Engineering University; Botanical Garden of Ural Branch of RAS. DOI: 10.13140/RG.2.2.31984.00001. *Retrieved from*: https://elar.usfeu.ru/bitstream/123456789/9647/2/Base1_v2_ob.pdf
[27] World Weather Maps, 2007. Retrieved from: https://www.mapsofworld.com/referrals/weather
[28] Usoltsev V A, Shobairi O, Tsepordey I S, Ahrari A, Zhang M, Shoaib A A and Chasovskikh V P 2020 Are there differences in the response of natural stand and plantation biomass to changes in temperature and precipitation? A case for two-needled pines in Eurasia. *Journal of Resources and Ecology*, **11** (4) 331-341 DOI: 10.5814/j.issn.1674-764x.2020.04.001
[29] Usoltsev V A, Zukow W, Osmirko A A, Tsepordey I S and Chasovskikh V P 2019b Additive biomass models for *Larix* spp. single-trees sensitive to temperature and precipitation in Eurasia. *Ecological Questions*, **30** (2) 57-67 DOI: http://dx.doi.org/10.12775/EQ.2019.012
[30] Usoltsev V A, Zukow W, Osmirko A A, Tsepordey I S and Chasovskikh V P 2019c Additive biomass models for *Quercus* spp. single-trees sensitive to temperature and precipitation in Eurasia. *Ecological Questions*, **30** (4) 29-40 (DOI: 10.12775/EQ.2019.021)
[31] Baskerville G L 1972 Use of logarithmic regression in the estimation of plant biomass. *Canadian Journal of Forest Research*, **2**(1) 49-53
[32] Poorter H, Jagodzinski A M, Ruiz-Peinado R, Kuyah S, Luo Y, Oleksyn J, Usoltsev VA, Buckley TN, Reich PB and Sack L 2015 How does biomass allocation change with size and differ among species? An analysis for 1200 plant species from five continents. *New Phytologist*, **208** (3) 736-749 (http://onlinelibrary.wiley.com/doi/10.1111/nph.13571/epdf)
[33] Usoltsev V A, Kovyazin V F, Osmirko A A, Tsepordey I S, Chasovskikh V P, Azarenok V A and Koltunova A I 2019d Model of root:shoot ratio in biomass of *Larix* spp. forests sensitive to winter temperature and mean precipitation in Eurasia. *Izvestia Sankt-PeterburgskojLesotehniceskojAkademii*, **229** 130–144 (DOI: 10.21266/2079-4304.2019.229.130-144)
[34] Wang W, Zu Y, Wang H, Matsuura Y, Sasa K and Koike T 2005 Plant biomass and productivity of *Larixgmelinii* forest ecosystems in northeast China: intra- and inter-species

comparison. *Eurasian Journal of Forest Research*, **8**(1): 21-41 URL: http://hdl.handle.net/2115/22188

[35] Schepaschenko D, Moltchanova E, Shvidenko A, Blyshchyk V, Dmitriev E, Martynenko O, See L and Kraxner F 2018 Improved estimates of biomass expansion factors for Russian forests *Forests*, **9** (6) 312 DOI: 10.3390/f9060312

[36] Ørka H O, Næsset E and Bollandsȧs O M 2009 Classifying species of individual trees by intensity and structure features derived from airborne laser scanner data. *Remote Sensing of Environment*, **113** 1163–1174

[37] Li W K, Guo Q H, Jakubowski M K and Kelly M 2012 A new method for segmenting individual trees from the lidar point cloud. *Photogrammetric Engineering & Remote Sensing*, **78** 75–84

[38] Kovyazin V F, Vinogradov K P, Kitcenko A A and Vasilyeva E A 2020 Airborne laser scanning for clarification of the valuation indicators of forest stands. *Lesnoy Zhurnal [Russian Forestry Journal]***6** 42–54 DOI: 10.37482/0536-1036-2020-6-42-54

[39] Holmgren J and Persson Å 2004 Identifying species of individual trees using airborne laser scanning. *Remote Sensing of Environment*, **90** 415-423

[40] Næsset E *et al* 2004 Laser scanning of forest resources: the Nordic experience. *Scandinavian Journal of Forest Research*, **19** 482-489

[41] Brandtberg T, Warner T A, Landenberger R E and McGraw J B 2007 Classifying individual tree species under leaf-off and leaf-on conditions using airborne lidar. *ISPRS Journal of Photogrammetry and Remote Sensing*, **61** (5) 325-340

[42] Li J, Hu B, Noland T L 2013 Classification of tree species based on structural features derived from high density LiDAR data. *Agricultural and Forest Meteorology*, **171** 104–114

[43] Blanchette D, Fournier R A, Luther J E and Côté J F 2015 Predicting wood fiber attributes using local-scale metrics from terrestrial LiDAR data: A case study of Newfoundland conifer species. *Forest Ecology and Management*, **347** 116-129

[44] Hasenauer H and Monserud R A 1996 A crown ratio model for Austrian forests. *Forest Ecology and Management*, **84** 49-60

[45] Oliver C D and Larson B C 1996 *Forest Stand Dynamics*. John Wiley & Sons, Inc., New York. p 520